Dual-bell nozzle for space launchers with fluidic control of transition

Dual-bell nozzle for space launchers with fluidic control of transition

Andrea Ferrero*
Politecnico di Torino, Torino, Italy, 10129

Antonietta Conte†
Politecnico di Torino, Torino, Italy, 10129

Emanuele Martelli ‡
Università degli Studi della Campania Luigi Vanvitelli, Aversa, Italy, 81031

Francesco Nasuti §
Sapienza Università di Roma, Roma, Italy, 00184

Dario Pastrone¶
Politecnico di Torino, Torino, Italy, 10129

The dual-bell nozzle is a promising altitude adaptive nozzle concept for improving the performance of existing space launchers as well as future reusable launch vehicles. It is characterized by an inflection in the wall geometry which links a base nozzle with a nozzle extension. Two working modes are therefore attained: a low-altitude mode in which the expansion is limited to the first bell and a high-altitude mode in which full expansion is achieved. Even though this capability makes it possible to reduce the non-adaptation losses in engines working from sea level to almost vacuum conditions, the natural transition between the two modes usually takes place prematurely during the ascent trajectory and destructive side-loads may arise. This results in a limitation on the performance gain. In this work, a dual-bell nozzle design capable of upgrading the parallel-staged Ariane 5 launcher is studied. Fluidic control is investigated as a possible solution to limit premature transition and reduce side-loads. The control is obtained by means of a secondary injection in the proximity of the inflection point: different injection strategies are investigated. Reynolds-averaged Navier–Stokes equations at steady state conditions are solved with an in-house CFD tool, to investigate the flow field and determine the required secondary mass flow rate and the range of nozzle pressure ratio for which the control is effective.

I. Nomenclature

$NPR = P_c/P_a$	=	Nozzle pressure ratio [-]
P_a	=	Ambient pressure [Pa]
P_c	=	Chamber total pressure [Pa]
P_w	=	Wall static pressure [Pa]
R_t	=	Throat radius [m]
x	=	Axial coordinate [m]
r	=	Radial coordinate [m]

*Assistant Professor, Department of Mechanical and Aerospace Engineering, Corso Duca degli Abruzzi 24, AIAA Member
†PhD Candidate, Department of Mechanical and Aerospace Engineering, Corso Duca degli Abruzzi 24, AIAA Student Member
‡Associate Professor, Department of Engineering, Via Roma 29
§Associate Professor, Department of Mechanical and Aerospace Engineering, Via Eudossiana 18, AIAA Member
¶Full Professor, Department of Mechanical and Aerospace Engineering, Corso Duca degli Abruzzi 24, AIAA Associate Fellow

II. Introduction

Ariane 5 is a parallel-staged European heavy lifter with a cryogenic main stage and two solid boosters that provide the majority of the lift-off thrust. For security reasons, the main stage engine, Vulcain 2, must be fired on the ground prior to igniting the solid boosters and launching the rocket. Due to this constraint, the main stage engine must operate in a wide variety of conditions, from sea level to near vacuum with consequent performance losses. To circumvent the area ratio limitation of conventional nozzles, several altitude adaptive nozzle concepts have been developed to increase the engine's overall specific impulse I_{sp} during the ascent trajectory [1–3], which allows for an increase in payload mass. This subsystem has therefore been identified as the one with the greatest potential for performance improvement.

The dual-bell nozzle has emerged as a potential solution to mitigate the non-adaptation losses observed in rocket engines. The main benefit of dual-bell nozzles over other methods of controlling nozzle separation is their simplicity, as there are no moving parts, and hence their great reliability. The presence of an inflection in the nozzle geometry enables two working modes: the flow expansion is limited to the first bell in the low-altitude mode, while full expansion is achieved in the high-altitude mode. Even though the concept itself has its advantages, there are side effects that have limited the widespread adoption of dual-bell nozzles to date. Side-loads can arise during transition due to oscillations of the separation line; these phenomena can generate asymmetrical distributions and lead to significant lateral forces [4]. Additionally, dual-bell nozzles switch from one operating mode to the other at a lower altitude than the one at which the full flow condition becomes more efficient. Several strategies have been investigated to control the transition, such as fluidic control [5–7], film cooling [8–10], and mixture ratio variation [10]. Fluidic control forces the separation line to the inflection point for a range of nozzle pressure ratio (NPR) higher than the reference NPR in the uncontrolled configuration. The growing demand for more affordable payload delivery, may find this concept as one of the primary game changers in the current space rocket market which foresees future reusable space launchers, due to the significant theoretical performance increase.

The purpose of this work is to demonstrate the feasibility of this technology for space launchers. The parallel-staged Ariane 5 was selected as a case study between existing space launchers, since it exemplifies the main stage engines' nozzle expansion ratio limitations. A dual-bell geometry, obtained by a parallel study in which both trajectory and nozzle were optimised, was investigated as potential alternative for the nozzle of the core engine: the effectiveness of fluidic control in increasing the transitional NPR and in limiting the displacement of the separation line was evaluated.

III. Physical model and numerical discretisation

The flow field inside the optimized dual-bell nozzle is modeled using Reynolds-averaged Navier-Stokes (RANS) equations, with the assumptions of 2-D axisymmetric, steady-state, compressible flow. An ideal gas with a specific heat ratio $\gamma = 1.14$ is assumed. The dynamic viscosity is evaluated by the Sutherland's law for water. The nozzle wall is considered adiabatic. The turbulence closure of the RANS equations is based on an adaptive version of the Spalart and Allmaras's model [7], which only applies a compressibility correction in the shear layer and has no effect on the production term in the boundary layer. A parallel in-house numerical code based on an unstructured discretization of the domain was adopted to integrate the governing equations [11]. The technique employed for discretization is the numerical method of lines; space is discretized using a second-order accurate unstructured finite volume scheme, while time is integrated using the linearized implicit Euler method. The spatial discretisation is accurate to the second order and the reconstruction required by convective fluxes is limited using the Barth-Jespersen technique [12], whereas the gradient required by diffusive fluxes and source terms is computed using the weighted least square method. Convective fluxes are evaluated using a hybrid solver [13] that combines Flux Difference Splitting [14, 15] and the local Lax-Friedrichs (or Rusanov) flux [16]. The computational domain is discretized using the Frontal-Delaunay for quads algorithm by the Gmsh tool [17]. The unstructured grid is managed in the parallel MPI environment via the DMPlex class [18] provided by the PETSc library [19].

IV. Results

The results of the numerical study are reported in this section. The geometry under investigation was obtained by a parametric study on an Ariane 5-like launcher in which both the trajectory and the dual-bell configuration were optimised. The area ratio for the base nozzle and the extension is 50 and 131, respectively. The chamber total temperature and total pressure are assumed to be equal to 3500 K and 115 bar, respectively. The throat radius is set at 0.137 m.
The simulations were performed on an unstructured mesh with approximately 180000 cells: the resolution was chosen after a preliminary mesh convergence analysis. In Section IV.A the flow field inside the uncontrolled nozzle for several

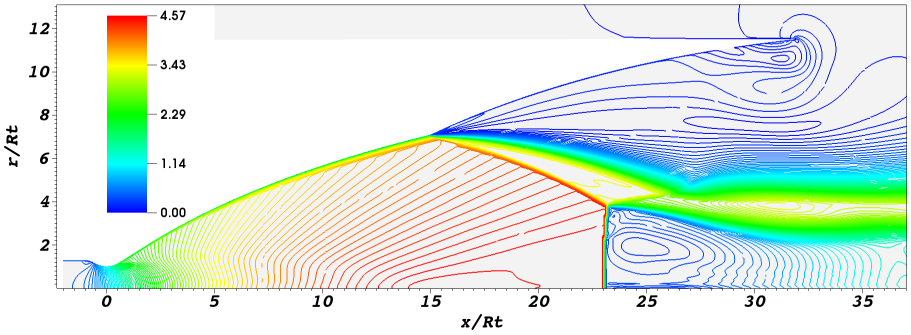

(a)

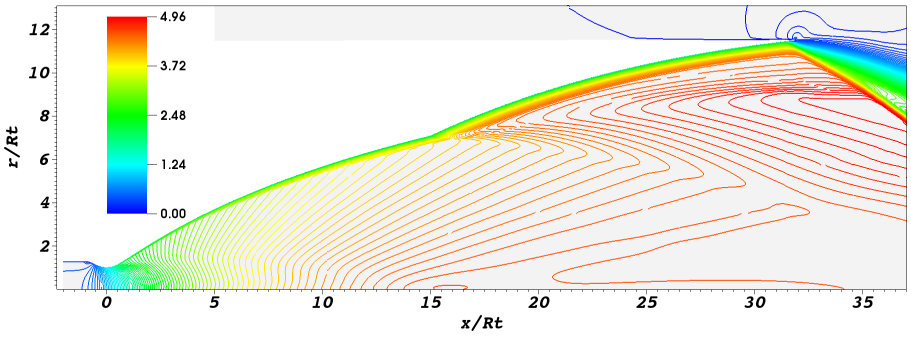

(b)

Fig. 1 Mach field at NPR=115 (a) and NPR=175 (b) without control.

values of nozzle pressure ratio (NPR) is described. In Section IV.B the study is repeated by introducing a secondary injection near the inflection point. Finally, a discussion on the influence of the injection Mach number is reported in Section IV.C.

A. Uncontrolled flow

The flow field in the uncontrolled dual-bell nozzle was simulated for several values of NPR, ranging from 115 to 175. The first value refers to the sea-level working condition and the Mach field is reported in Figure 1a: the separation is located at the inflection point ($x/R_t = 15$). The NPR was then increased and a full flow working condition was first obtained at NPR=175. The Mach field at NPR=175 is reported in Figure 1b.

The wall pressure distribution for several values of NPR is reported in Figure 2. The results show clearly that the shock-induced separation predicted by the RANS simulations moves downstream as the NPR is increased: it finally jumps to the end of the second bell for NPR>170. It is possible to observe that the separation line shows significant displacements in the inflection region for a relatively large NPR range (115<NPR<170): this behaviour can be associated to the development of potential side-loads during the uncontrolled transition.

B. Controlled flow

A second set of simulations was performed by introducing a secondary injection from a slot located at $x/R_t = 16$. The width of the slot was set to 1 cm. The total temperature and total pressure of the injected fluid were assumed equal to 300 K and 1.96 bar, respectively. The injection is supersonic ($M_i = 2$) and it is performed radially. The injected gas is supposed to have the same specific heat ratio as the fluid from the main chamber. As a result, the mass flow rate of the secondary injection represents 3.15% of the mass flow rate from the combustion chamber. The properties of the secondary injection were chosen after a preliminary study on the flow field generated by the interaction between the

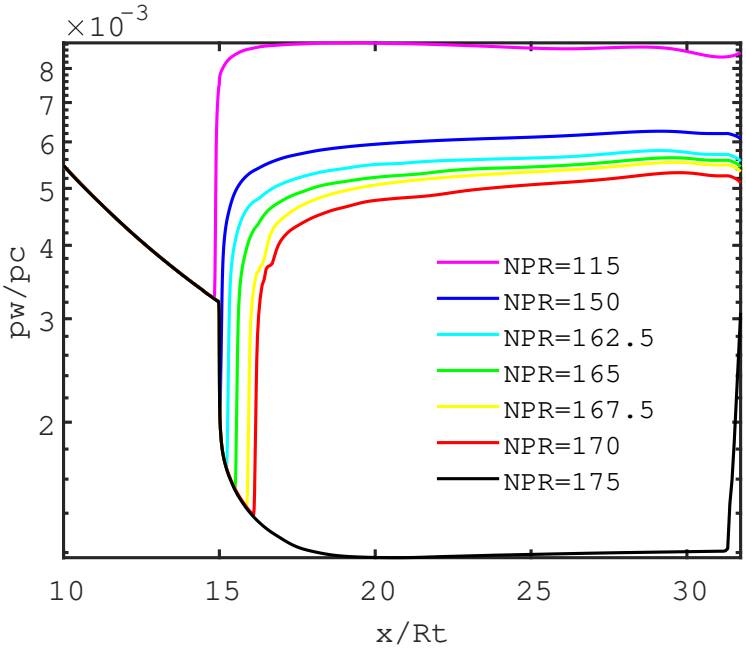

Fig. 2 Wall pressure distribution in the optimized dual-bell nozzle for 115<NPR<175 without control.

primary flow and the secondary jet. A discussion on the influence of the injection Mach number is reported in Section IV.C.

The flow field obtained by the introduction of the secondary injection was investigated for 175<NPR<220. The Mach field at NPR=175 with the secondary injection is reported in Figure 3a. It is interesting to compare this result with the Mach field at NPR=175 in the uncontrolled nozzle (see Figure 1): while the uncontrolled flow is fully reattached, the injection keep the separation at the inflection point ($x/R_t = 15$). A detail of the Mach field is reported in Figure 4: the injected fluid keeps the separated shear layer far from the wall and prevent reattachment.

As the NPR is increased, the separation line shows small displacements from the inflection point: the secondary injection seems capable of keeping the separation anchored to the inflection point for a significant NPR range. This is a promising result since the side-loads are usually observed when the separation line moves in the inflection region during the natural transition.

The effectiveness of the secondary injection stops when the NPR is increased beyond 200. For higher values of NPR, the injection is still able to induce a small separation but then the flow reattaches just downstream to the injection slot. An example of this flow configuration is reported for NPR=220 in Figure 3b.11

It is possible to see the evolution of the wall pressure distribution as the NPR is increased in Figure 5. Finally, the separation location as a function of the NPR is reported in Figure 6 for both the uncontrolled and controlled configurations. This plot summarises the results of the present work: the introduction of a secondary injection is able to significantly increase the transitional NPR with respect to the uncontrolled configuration. Furthermore, the injection is able to anchor the separation to the inflection point for a relatively large range of NPR. These results suggest that it would be convenient to keep the injection active from sea-level up to the altitude where NPR=200 is reached: if the injection is deactivated at NPR=200 then the separation line moves immediately to the end of the nozzle because this NPR is significantly larger than the natural transitional NPR. In this way it could be possible to limit the transition duration and the potential development of side-loads.

C. Influence of injection Mach number

In this section, the influence of the injection Mach number is discussed. The total pressure of the secondary injection was chosen sufficiently large to guarantee choked flow in the injection slot at sea level. A first set of simulations were performed assuming sonic injection through a slot located at the injection point ($x/R_t = 15$). However, when the NPR increases, the jet emitted by the slot becomes strongly underexpanded. As a result, the secondary flow continues its

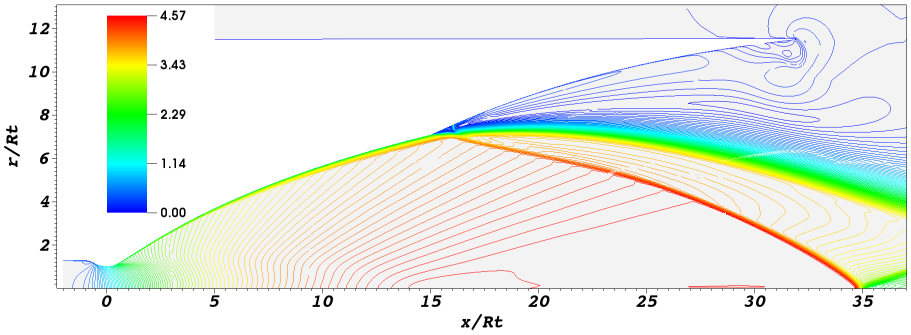

(a)

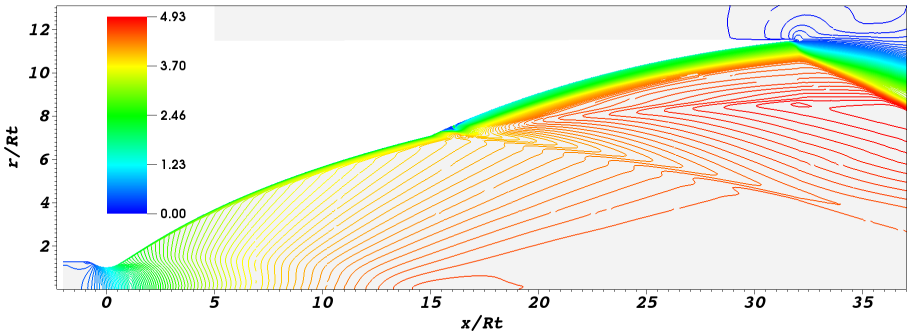

(b)

Fig. 3 Mach field at NPR=175 (a) and NPR=220 (b) with control.

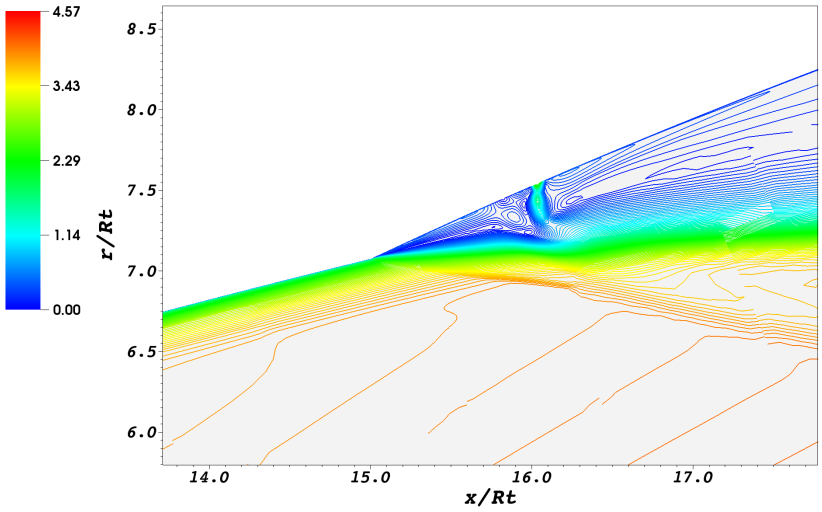

Fig. 4 Mach field at NPR=175 with control: detail of the injection region.

expansion when it is introduced into the nozzle. This can lead to problems related to the reattachment of the separated flow. An example of this behaviour can be observed at NPR=165. The Mach field obtained by performing a sonic injection in the wall normal direction is reported in Figure 7. The figure shows also some streamlines which identify

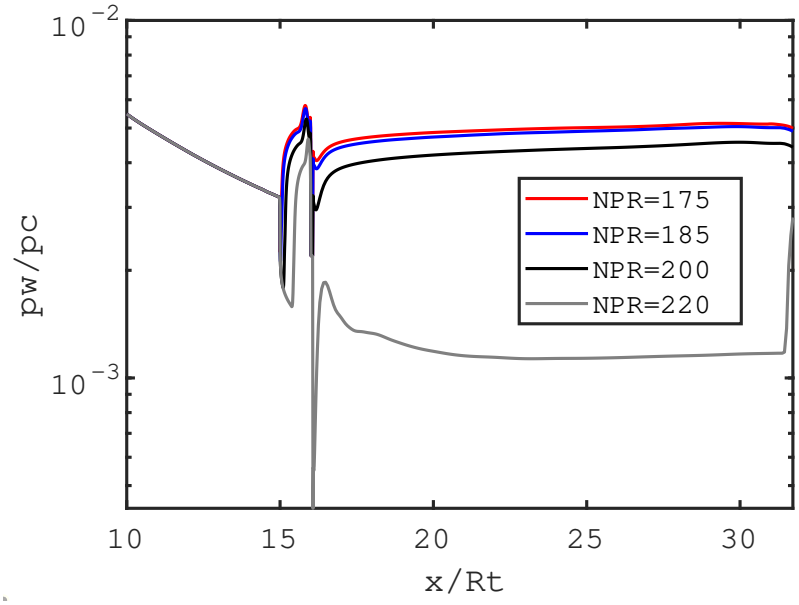

Fig. 5 Wall pressure distribution in the optimized dual-bell nozzle for 115<NPR<175 with secondary injection.

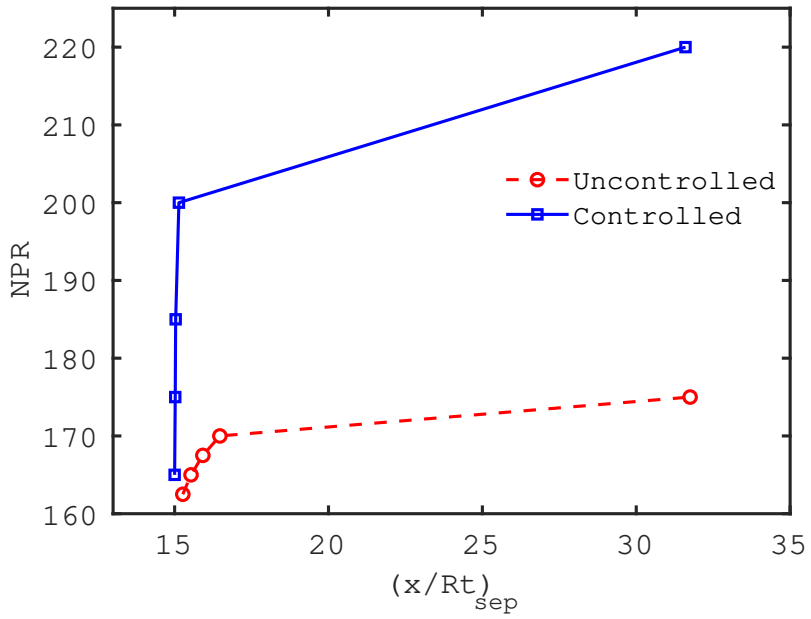

Fig. 6 Separation location at different NPRs for uncontrolled and controlled flow.

the streamtube coming out from the injection slot. The plot shows clearly that this streamtube expands significantly and, doing so, induces the reattachment of the flow. However, a second uncontrolled separation is observed further downstream: this configuration could be potentially affected by side-loads generated by the oscillation of the second separation line and so the fluidic control does not appear effective in this case.

An alternative approach was investigated by considering a supersonic injection at $M_i = 2$ in the radial direction. The Mach field and some streamlines obtained by this strategy at NPR=165 are reported in Figure 8. In this case the secondary jet is overexpanded and it does not induce the reattachment.

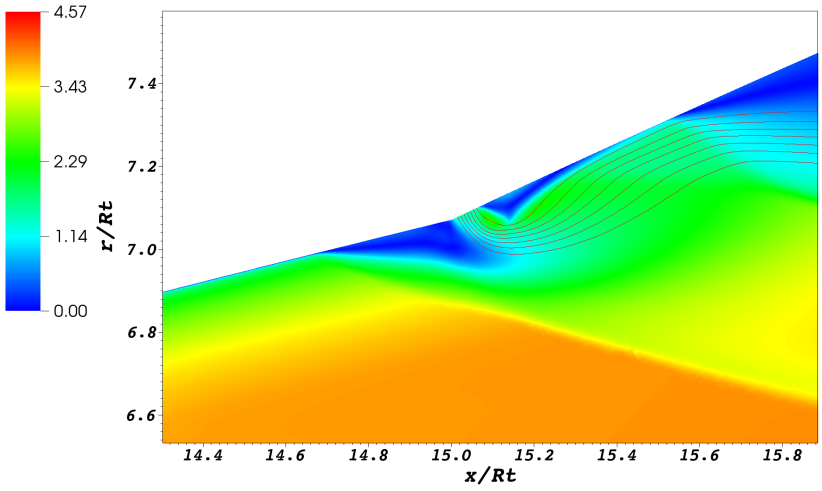

Fig. 7 Mach field and streamlines in the inflection region (sonic injection in the wall normal direction at $x/R_t = 15$).

This preliminary study was conducted with the injection at $x/R_t = 15$. As can be seen in both Figures 7 and 8, the separation induced by the injection moves upstream in the first bell. This result suggests moving the injection slot downstream with respect to the inflection point in order to exploit the inflection point as an anchor for the separation. For this reason, all the results reported in Section IV.B were obtained by placing the injection slot at $x/R_t = 16$.

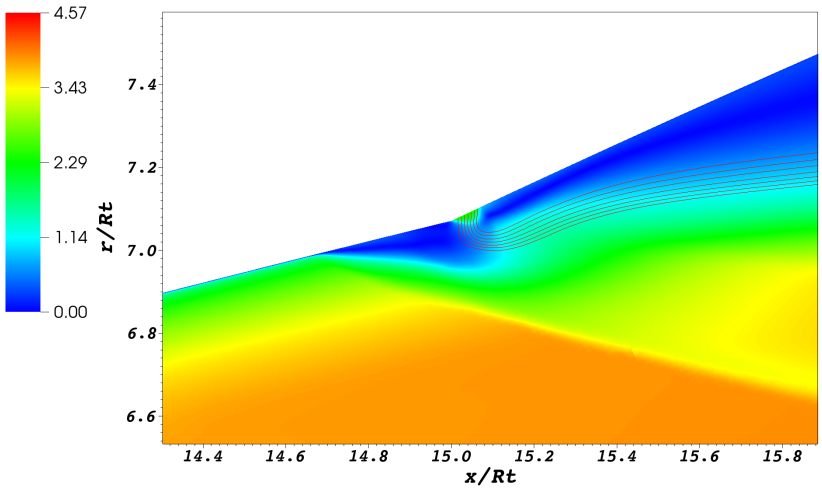

Fig. 8 Mach field and streamlines in the inflection region (supersonic $M_i = 2$ radial injection at $x/R_t = 15$).

V. Conclusion

The flow field in a dual-bell nozzle was studied by means of RANS simulations. The potential of fluidic control was investigated for increasing the transitional NPR. The numerical results showed that a secondary injection with a mass

flow rate equal to 3.15% of the chamber mass flow rate can significantly increase the transitional NPR (from 170 to 200). Furthermore, the secondary injection strongly limits the displacement of the separation line as the NPR is increased. These two findings suggest that fluidic control is a promising strategy to limit side-loads during transition: the secondary injection should remain active until a sufficiently large NPR is reached during the ascent trajectory (NPR=200 in this case). If the secondary injection is deactivated at this altitude, then the separation line jumps from the inflection point to the end of the nozzle. In this case, the separation line is not allowed to move from the inflection point until the injection is deactivated. This reduces the time during which side loads could develop with respect to the uncontrolled configuration: in the uncontrolled flow the separation line shows significant displacements in the inflection regions as the NPR increases and these displacements can be related to potential side-loads.
A preliminary investigation put in evidence the importance of the injection Mach number: in particular, a strongly underexpanded jet should be avoided because it could induce a reattachment followed by an uncontrolled separation.
In conclusion, the secondary injection considered in this work was performed by means of a cold gas (T=300 K) at low pressure (1.96 bar): the gas could be provided by a dedicated tank with a pressure regulator. However, the relatively low mass flow rate (3.15% of the chamber mass flow rate) allows to consider several alternatives. For example, the secondary mass flow rate could be obtained by the turbine exhaust of an open-cycle engine.

Acknowledgments

Computational resources were provided by HPC@POLITO, a project of Academic Computing within the Department of Control and Computer Engineering at the Politecnico di Torino (http://www.hpc.polito.it).

References

[1] Hagemann, G., Immich, H., Van Nguyen, T., and Dumnov, G. E., "Advanced rocket nozzles," *Journal of Propulsion and Power*, Vol. 14, No. 5, 1998, pp. 620–634.

[2] Frey, M., and Hagemann, G., "Critical assessment of dual-bell nozzles," *Journal of propulsion and power*, Vol. 15, No. 1, 1999, pp. 137–143.

[3] Nasuti, F., Onofri, M., and Martelli, E., "Role of wall shape on the transition in axisymmetric dual-bell nozzles," *Journal of propulsion and power*, Vol. 21, No. 2, 2005, pp. 243–250.

[4] Cimini, M., Martelli, E., and Bernardini, M., "Numerical Analysis of Side-loads Reduction in a Sub-scale Dual-bell Rocket Nozzle," *Flow, Turbulence and Combustion*, 2021, pp. 1–24.

[5] Tomita, T., Takahashi, M., and Sasaki, M., "Control of transition between two working modes of a dual-bell nozzle by gas injection," *45th AIAA/ASME/SAE/ASEE Joint Propulsion Conference & Exhibit*, 2009, p. 4952.

[6] Zmijanovic, V., Leger, L., Sellam, M., and Chpoun, A., "Assessment of transition regimes in a dual-bell nozzle and possibility of active fluidic control," *Aerospace Science and Technology*, Vol. 82, 2018, pp. 1–8.

[7] Ferrero, A., Martelli, E., Nasuti, F., and Pastrone, D., "Fluidic control of transition in a dual-bell nozzle," *AIAA Propulsion and Energy 2020 Forum*, 2020, p. 3788.

[8] Martelli, E., Nasuti, F., and Onofri, M., "Film cooling effect on dual-bell nozzle flow transition," *45th AIAA/ASME/SAE/ASEE Joint Propulsion Conference & Exhibit*, 2009, p. 4953.

[9] Proschanka, D., Yonezawa, K., Koga, H., Tsujimoto, Y., Kimura, T., and Yokota, K., "Control of operation mode transition in dual-bell nozzles with film cooling," *Journal of Propulsion and Power*, Vol. 28, No. 3, 2012, pp. 517–529.

[10] Schneider, D., Stark, R., Génin, C., Oschwald, M., and Kostyrkin, K., "Active Control of Dual-Bell Nozzle Operation Mode Transition by Film Cooling and Mixture Ratio Variation," *Journal of Propulsion and Power*, Vol. 36, No. 1, 2020, pp. 47–58.

[11] Conte, A., Ferrero, A., Larocca, F., and Pastrone, D., "Numerical Tool Optimization for Advanced Rocket Nozzle Performance Prediction," *AIAA Propulsion and Energy 2019 Forum*, 2019, p. 4115.

[12] Barth, T., and Jespersen, D., "The design and application of upwind schemes on unstructured meshes," *27th Aerospace sciences meeting*, 1989, p. 366.

[13] Ferrero, A., and D'Ambrosio, D., "A hybrid numerical flux for supersonic flows with application to rocket nozzles," *Advances in Aircraft and Spacecraft Science*, Vol. 7, No. 5, 2020, pp. 387–404.

[14] Osher, S., and Solomon, F., "Upwind difference schemes for hyperbolic systems of conservation laws," *Mathematics of computation*, Vol. 38, No. 158, 1982, pp. 339–374.

[15] Pandolfi, M., "A contribution to the numerical prediction of unsteady flows," *AIAA journal*, Vol. 22, No. 5, 1984, pp. 602–610.

[16] Rusanov, V. V., "The calculation of the interaction of non-stationary shock waves and obstacles," *USSR Computational Mathematics and Mathematical Physics*, Vol. 1, No. 2, 1962, pp. 304–320.

[17] Geuzaine, C., and Remacle, J.-F., "Gmsh: A 3-D finite element mesh generator with built-in pre-and post-processing facilities," *International journal for numerical methods in engineering*, Vol. 79, No. 11, 2009, pp. 1309–1331.

[18] Lange, M., Knepley, M. G., and Gorman, G. J., "Flexible, scalable mesh and data management using PETSc DMPlex," *Proceedings of the 3rd International Conference on Exascale Applications and Software*, University of Edinburgh, 2015, pp. 71–76.

[19] Balay, S., Abhyankar, S., Adams, M., Brown, J., Brune, P., Buschelman, K., Dalcin, L., Dener, A., Eijkhout, V., Gropp, W., et al., "PETSc users manual," 2019.